Influence of Trp Mutation on Native, Intermediate, and Transition States of Goat α-Lactalbumin: An Equilibrium and Kinetic Study

A. Chedad, H. Van Dael,* A. Vanhooren, and I. Hanssens

Interdisciplinary Research Centre, K. U. Leuven Campus Kortrijk, B-8500 Kortrijk, Belgium

Received June 28, 2005; Revised Manuscript Received September 21, 2005

ABSTRACT: Equilibrium circular dichroism and kinetic stopped-flow fluorescence studies on the stability and the folding kinetics of a set of Trp to Phe mutants of goat α-lactalbumin (GLA) were used to characterize the native, intermediate, and transition states of these constructs. GLA contains four tryptophan residues, three of which, Trp26, Trp104, and Trp118, are located in the α-domain, while the fourth, Trp60, is located in the *β*-domain. Trp26, Trp60, and Trp104 are part of a hydrophobic cluster, whereas Trp118 is situated in a more flexible region near the C-terminal end of the protein. In each case, the mutation leads to a reduction in the overall stability, but only for W26F and W60F is an equilibrium intermediate observed in guanidine hydrochloride-induced unfolding experiments. In kinetic refolding experiments, however, for all samples a burst phase is observed, the amplitude of which depends on the specific mutation. Refolding and unfolding kinetics can adequately be described by a sequential three-state mechanism. *ϕ* value analysis showed that the local structure around Trp26, Trp60, and Trp104 is formed in the intermediate and in the transition state of the folding reaction, while around Trp118 no persistent native contacts are observed. From these findings, we conclude that, although hydrophobicity is a major driving force for folding, minor steric changes induced by point mutation can considerably influence the overall stability and the folding process of the protein.

Many proteins populate partially structured intermediates while folding from the unfolded to the native state (*1*, *2*). Although the folding pathways of these proteins have been studied intensively, the debate about the nature of these intermediate states, their role in the folding process, and their possible similarity with intermediate states populated under equilibrium conditions continues (*3*−*5*). Specific questions about the heterogeneity and stability of these intermediate states remain, and the place and the height of the energy barriers that separate these states from the native and unfolded states are often unknown. Therefore, we performed a systematic study of the influence of point mutations on the stability and kinetics of the different states that occur during the folding and unfolding of goat α-lactalbumin.

α-Lactalbumin is a small globular protein of 123 amino acids that acts as a regulatory subunit of the lactose synthase system. The structure of α-LA is made up of a large α-helical domain (residues 1−39 and 85−123) and a small *β*-sheet domain (residues 40−84) which are connected by a calcium-binding loop (Figure 1) (*6*, *7*). The α-helical domain comprises four major α-helices and a short 3_{10}-helix. The *β*-domain is composed of a three-stranded antiparallel *β*-sheet, a loop structure, and a short 3_{10}-helix. All α-lactalbumins investigated thus far, including the goat protein (GLA),[1] form a molten globule state under a variety of conditions such as low pH, moderate denaturant concentration, and depletion of Ca^{2+} ions (*8*, *9*). GLA possesses four tryptophans at positions 26, 60, 104, and 118 (Figure 1). Trp26, Trp104, and Trp118 are in the α-domain of the protein. Their position in that domain, however, is different.

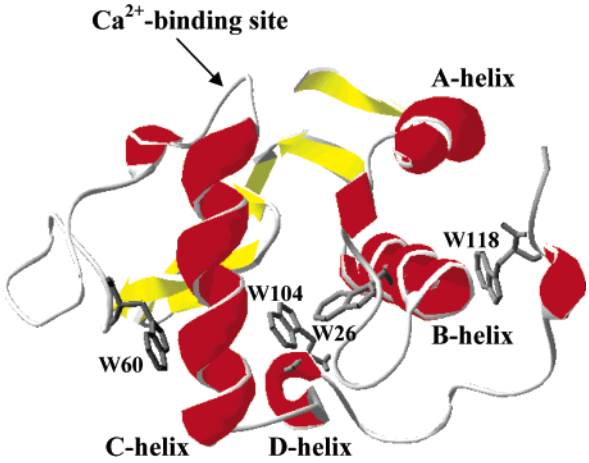

FIGURE 1: Crystal structure of goat LA generated from coordinates deposited in the Protein Data Bank [entry 1HFY (*7*)] using SWISS-MODEL (*47*). The side chains of the four Trp residues are represented by sticks. Helices are colored red, and the *β*-sheet is colored yellow. The arrow indicates the Ca^{2+}-binding site with Lys79, Asp82, Asp84, Asp87, and Asp88 as ligands.

* To whom correspondence should be addressed: Interdisciplinary Research Centre, K. U. Leuven Campus Kortrijk, E. Sabbelaan 53, B-8500 Kortrijk, Belgium. Telephone: +32-56-246111. Fax: +32-56-246997. E-mail: herman.vandael@kulak.ac.be.

[1] Abbreviations: GLA, goat α-lactalbumin; wt, wild type; W118F, W104F, W60F, and W26F, mutants of GLA in which Trp118, Trp104, Trp60, and Trp26, respectively, are replaced with phenylalanine; GdnHCl, guanidine hydrochloride; c_M, GdnHCl concentration at the transition midpoint; CD, circular dichroism; UV, ultraviolet; N, I, and U, native, intermediate, and unfolded states of the protein, respectively; TS, transition state; Tris, tris(hydroxymethyl)aminomethane.

10.1021/bi0512400 CCC: $30.25
Published on Web 10/29/2005

Trp118 is situated in a more flexible region near the C-terminal end of the protein and forms aromatic cluster I together with Phe31 and His32. Trp26 and Trp104 are part of the so-called hydrophobic box or aromatic cluster II together with Tyr103 in the α-domain and Phe53 and Trp60 in the β-domain.

From stopped-flow fluorescence and circular dichroism measurements, it is well-known that during refolding α-LA exhibits a kinetic intermediate which accumulates within the first milliseconds giving rise to an apparent burst phase (*10*, *11*). This early kinetic intermediate is compact and contains extensive and fixed secondary structure but has fluctuating tertiary interactions. It thus resembles the partially folded molten globule found under equilibrium conditions (*8*, *12*). Such a partially folded kinetic intermediate has been observed for many proteins, and different techniques such as NMR and hydrogen exchange have been used for the structural characterization of this transient intermediate (*13*). An alternative way to monitor specific individual interactions in transiently formed folding intermediates is given by the analysis of the changes in kinetics induced by specific mutations in the protein (*14*−*17*). We adopted the latter method for GLA in which each of the Trp residues in turn was changed to Phe. The kinetics of the wild-type protein and the influence of environmental conditions such as pH and Ca^{2+} binding were examined previously (*18*). In this work, we report on how a single Trp to Phe mutation affects the stability of the kinetic intermediate, the transition state, and the native state. By stopped-flow fluorescence experiments and ϕ value analysis, we furthermore have tried to discriminate between the influence of a mutation in the hydrophobic core and that of a mutation at the protein surface.

The results indicate that the kinetic intermediate states of the various mutants exhibit different stabilities. Furthermore, there is a strong correlation between the stability of the kinetic intermediate state and that of the native state. The energy level of the transition state, however, is much less affected by the location of the mutation site. Modeling of the kinetic results leads to the conclusion that the native and kinetic intermediate states of the W26F mutant are severely destabilized. Our result suggests that, although hydrophobicity is an important driving force for folding, it is not the only factor that leads to native tertiary contacts. The steric specificity of the amino acid is also a determinant for the stability of the kinetic intermediate and for the way in which the final native structure is established.

MATERIALS AND METHODS

Construction of Wild-Type GLA and Single-Trp Mutants of GLA. Recombinant GLA and its Trp mutants were expressed in *Pichia pastoris.* This expression system secretes native GLA without the extra N-terminal methionine which is present in the production with *Escherichia coli*. This is of major importance as it has been shown that methionyl-LA has more solvent accessible Trp residues, a lower stability, and a decreased calcium affinity compared to the authentic protein (*19*, *20*). Furthermore, the wild-type protein expressed in *P. pastoris* has been shown to possess spectroscopic properties identical to those of GLA from milk whey (*21*). The latter reference also contains the details on the construction, expression, and purification of the GLA mutants with a single Trp exchanged for Phe. A substitution with Phe has been chosen because of its hydrophobic character and its rather low fluorescence relative to that of either tryptophan or tyrosine. Moreover, in various proteins, it has been demonstrated that this substitution can be effectuated with conservation of the overall conformation (*22*, *23*).

Equilibrium Circular Dichroism Experiments. Circular dichroism measurements were carried out on a Jasco J-600A spectropolarimeter using cuvettes with a path length of 1 cm in the near-UV region and of 1 mm in the far-UV region. The data were expressed as molar ellipticity [θ] (degree square centimeter per decimole). The protein concentration was ∼0.3 mg/mL. Before a spectrum was recorded, the protein samples were left to equilibrate at 25 °C for 10 min in the presence of various GdnHCl concentrations. Unless mentioned otherwise, all experiments were conducted in 20 mM Tris, 10 mM Ca^{2+}, and 80 mM Na^{+} at pH 7.5.

Kinetic Experiments. Fluorescence folding and unfolding experiments were performed on a SX.18MV sequential mixing stopped-flow spectrometer from Applied Photophysics (Leatherhead, U.K.). The stopped-flow unit and the observation cell with a path length of 2 mm were thermostated with circulating water from a temperature-controlled bath. A monochromator was used for excitation at 280 nm and, the fluorescence emission was measured using a high-pass filter with a 320 nm cutoff. The dead time of the instrument was estimated to be ∼2 ms. Kinetic traces were measured 10−12 times, averaged, and analyzed as a sum of exponential functions by using the manufacturer's software. The initial protein concentration was ∼1.3 mg/mL. After the protein was mixed with buffer in a 1/10 ratio, this leads to a final concentration of ∼0.12 mg/mL in the cell.

Thermodynamic Analysis of the Equilibrium Unfolding Data. For a two-state transition, the observed signal S_{obs} can be expressed as a function of the denaturant concentration c by the following equation (*24*):

$$S_{obs}(c) = \frac{S_N + S_U \exp[-(\Delta G_{NU}^{H_2O} - m_{NU}c)/RT]}{1 + \exp[-(\Delta G_{NU}^{H_2O} - m_{NU}c)/RT]} \quad (1)$$

where $\Delta G_{NU}^{H_2O}$ is the Gibbs free energy difference between the native and unfolded state in 0 M GdnHCl and m_{NU} is the cooperativity index of the transition. We further assume that S_N and S_U vary linearly with denaturant concentration.

For the proteins that exhibit a three-state transition, we used a more complex variant of eq 1, in which the population of the intermediate state is explicitly taken into account (*25*, *26*):

$$S_{obs}(c) = \frac{S_N + S_I \exp[-(\Delta G_{NI}^{H_2O} - m_{NI}c)/RT] + S_U \exp[-(\Delta G_{NU}^{H_2O} - m_{NU}c)/RT]}{1 + \exp[-(\Delta G_{NI}^{H_2O} - m_{NI}c)/RT] + \exp[-(\Delta G_{NU}^{H_2O} - m_{NU}c)/RT]} \quad (2)$$

In this expression, the observed signal $S_{obs}(c)$ at any GdnHCl concentration is the weighted sum of the individual contributions originating from the N, I, and U states, respectively.

The CD and fluorescence data were analyzed by global fitting using eq 2 with $\Delta G_{NI}^{H_2O}$, $\Delta G_{NU}^{H_2O}$, m_{NI}, and m_{NU} as

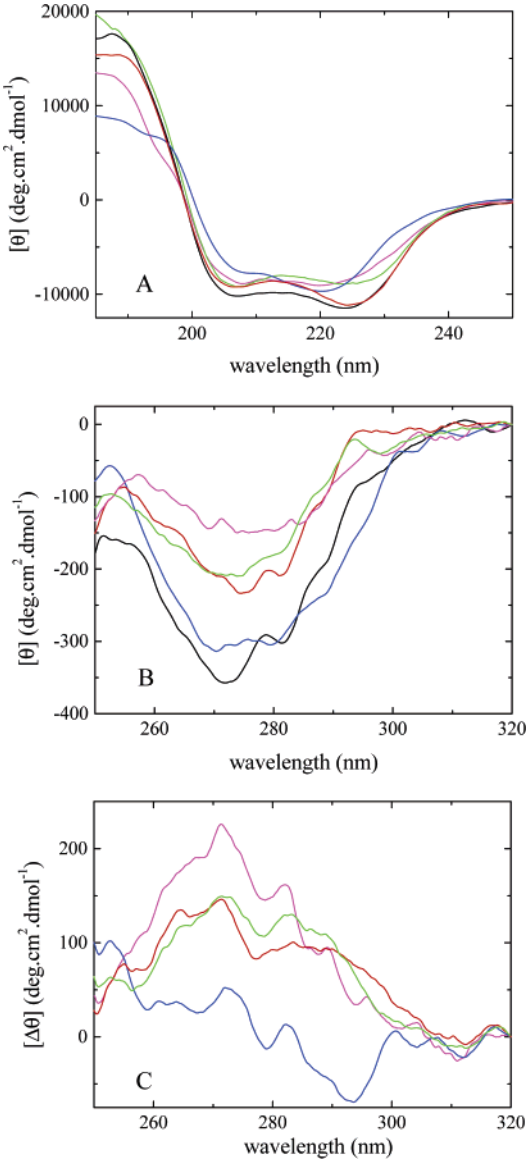

FIGURE 2: (A) Far-UV and (B) near-UV CD spectra of wild-type GLA (black), W118F (red), W104F (magenta), W60F (blue), and W26F (green) at pH 7.5 and 25 °C. The difference spectra (mutant minus wild type) are shown in panel C. These spectra were recorded in 10 mM Tris and 2 mM Ca^{2+}.

fitting variables. In the analysis, we initially set S_I equal to S_U for the fluorescence and CD measurements at 270 nm and S_I equal to S_N for the experiments at 222 nm.

RESULTS

Circular Dichroism Spectra. Figure 2 shows the far- and near-UV CD spectra of wild-type GLA and the four Trp mutants in the native state at 25 °C. In the far-UV region, the effects of the mutation on the CD spectrum are very limited. The overall shape and the pronounced negative ellipticity with double minima between 200 and 230 nm are conserved for all the proteins, referring to the same secondary structure. The spectra differ mostly in the 220−230 nm region. In that wavelength region, aromatic side chains could complement the dominant contribution of the α-helices to the spectrum (*27*). The depth of the shoulder around 230 nm is unaffected when Trp118 is replaced but diminishes gradually when in turn Trp26, Trp104, and finally Trp60 are mutated to Phe.

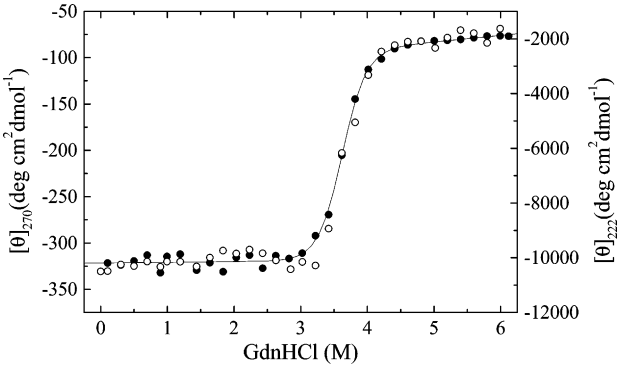

FIGURE 3: Equilibrium chemical denaturation of wild-type GLA. The ellipticity at 222 (○) and 270 nm (●) is plotted as a function of GdnHCl concentration. The solid line is the fit that results from the two-state model with the parameters from Table 1.

The most remarkable feature in the near-UV spectrum of all lactalbumins is the deep trough near 270 nm. Its amplitude, being the largest for wild-type GLA with four Trp residues, diminishes whenever a Trp residue is mutated. Figure 2B shows that this decrease strongly depends on which Trp is replaced. The strongest reduction is observed in W104F and the smallest one in W60F. The difference spectra (mutant minus wild type) for the different constructs of GLA are shown in Figure 2C. Such a difference spectrum can be expected to reveal the net contribution of each mutated tryptophan to the total near-UV CD spectrum of the wild-type protein. All these difference spectra exhibit clear peaks at 271 and 282 nm which are known as the tryptophan bands in the CD spectrum. The contribution of each of the three Trp residues situated in the α-domain is more important than that of Trp60 situated in the *β*-domain. Trp118 and Trp26 contribute in a nearly equal manner, and Trp104 has the largest CD band at 271 nm and is thus responsible for the major contribution in the near-UV CD spectrum of the protein. Trp60 which has the slightest contribution in the overall spectrum has a clear positive band at 293 nm.

Equilibrium Unfolding Studies. Equilibrium unfolding CD data at 222 and 270 nm were obtained for wt GLA, W118F, W104F, W60F, and W26F at pH 7.5 and 25 °C (Figures 3 and 4). As reported previously, the unfolding of recombinant wild-type GLA is identical with that of authentic GLA derived from milk (*28*). The midpoint of the transition is situated at 3.63 M. In accordance with the results of Chaudhuri et al. (*20*), our wild-type GLA is considerably more stable (42.84 kJ/mol compared to 25.91 kJ/mol) than that used in other experiments, where the wild-type GLA contains an extra methionine at the C-terminus (*26*). The transition curves obtained at 222 and 270 nm are completely coincident within experimental error (Figure 3), supporting our previous conclusion that the GdnHCl-induced equilibrium unfolding of GLA is purely two-state (*18*). This is also the case for the W104F and W118F mutants (not shown). For wt GLA, W104F, and W118F, our experimental data observed at 222 and 270 nm (Figure 3) perfectly fit the theoretical curve obtained by a nonlinear least-squares method using eq 1. The resulting values of the thermodynamic parameters $\Delta G_{NU}^{H_2O}$ and m_{NU} are listed in Table 1. The stability of W104F, however, has decreased by 9.50 kJ/mol, but it is not affected by the W118F mutation. Whereas the effect of the replacement of Trp118, situated near the

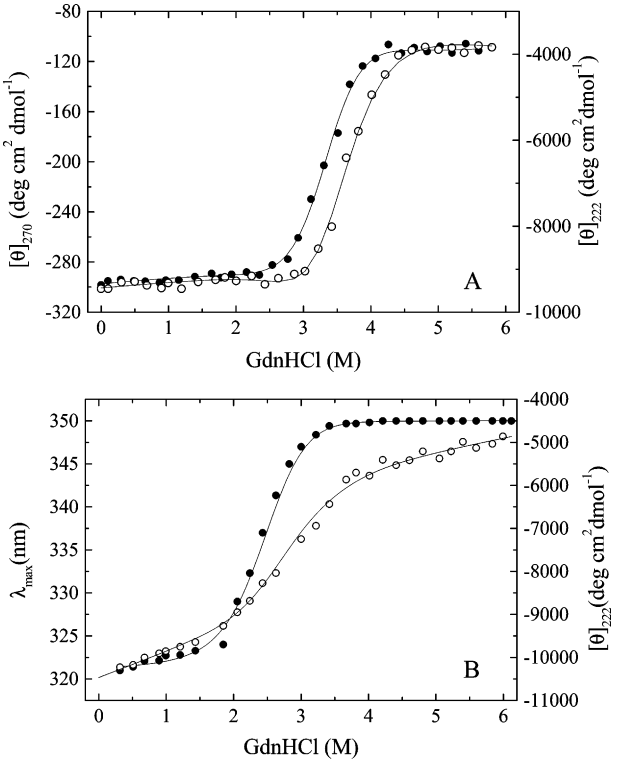

FIGURE 4: GdnHCl-induced equilibrium unfolding transition of W60F (A) and W26F (B) measured by the CD ellipticity at 222 (○) and 270 nm (●) for the W60F mutant and by the CD ellipticity at 222 nm (○) and the shift of the wavelength maximum (●) of the fluorescence for the W26F mutant. The solid line that fits the data points results from the equilibrium three-state model with the parameters listed in Table 1.

C-terminus, is rather limited, the replacement of Trp104, which belongs to the hydrophobic box, is more drastic. In contrast with the unfolding behavior of the former proteins, the transitions observed upon the unfolding of the secondary and tertiary structure no longer coincide for W60F and W26F (Figure 4). For W60F, the CD signal measured at 270 nm has a markedly lower transition midpoint than the CD curve measured at 222 nm, indicating that the disruption of tertiary structure precedes the loss of secondary structure and gives rise to one or more partially folded intermediate states. Similarly for W26F, the fluorescence transition curve and the far-UV CD transition curve are clearly uncoupled. In this case, the secondary structure unfolding extends over a broad concentration range with a midpoint at 2.81 M.

For the analysis of the unfolding transition of W26F and W60F, eq 2 was used with $\Delta G_{NI}^{H_2O}$, $\Delta G_{NU}^{H_2O}$, m_{NI}, and m_{NU} as fitting variables. The results are also listed in Table 1. The theoretical curves drawn with the obtained parameter values fit very well our experimental data (Figure 4), and the equilibrium transition of W26F and W60F, therefore, can be excellently described by the three-state model.

Folding and Unfolding Kinetics. Figure 5A shows the kinetic refolding traces obtained in a stopped-flow fluorescence experiment with a refolding buffer leading to a final concentration of 0.54 M GdnHCl.

The traces plotted in Figure 5A are normalized with as reference the fluorescence intensity of the unfolded protein under refolding conditions (0.54 M GdnHCl), and they show that a substantial intensity change occurs within the dead time (2 ms) of the stopped-flow experiment. This signal loss, also called burst phase amplitude, varies strongly, from 6 to 55%, depending on the specific mutant.

The observable part of the signal can best be fitted to a three-exponential function. For each of the proteins, however, the amplitude of the third phase is so small (less than 2.5%) that it will be omitted. In a biexponential analysis, the two rate constants k_1 and k_2 for the wt protein amount to 20.8 ± 0.5 and 2.06 ± 0.1 s^{-1}, respectively, with fractional amplitudes of 90.4 and 9.6% of the observed intensity change, respectively (Table 2). The mutation of Trp118 leaves these parameters practically unchanged, and the mutation of Trp26 hardly influences the rate constants. Substitution of Trp60, however, reduces k_1 to 11.9 ± 0.5 s^{-1} without a significant change in k_2 or in the contributions of the respective amplitudes. In W104F, finally both rate constants have increased.

In Figure 5B, the normalized fluorescence intensity during the unfolding process to a final GdnHCl concentration of 5.05 M is depicted. For all samples, the evolution toward the unfolded state, the fluorescence of which has been set to 1, can be described by a single-exponential function (Table 2). Mutation of Trp118, Trp104, and Trp26 causes increases in the unfolding rate constant of factors of 2, 7, and 100, respectively, while the replacement of Trp60 has practically no effect. None of the samples shows a fluorescence intensity change during the dead time, and except for W26F, the unfolding rate constant is lower than the refolding rate constant.

In general, when a protein unfolds, Trp residues become more and more water accessible, and therefore, the intensity of the fluorescence emission of the protein decreases due to a higher rate of internal conversion (*29*). In GLA and its Trp mutants, we observe just the opposite: the intensity in the unfolded state increases with respect to the intensity in the native state due to a very important loss of internal quenching. In absolute terms, the fluorescence intensity change during refolding is the largest in wild-type GLA, the fluorescence of which is largely quenched in the native state as has been concluded previously from static fluorescence spectra (*21*).

Dependence on GdnHCl Concentration and Chevron Plots. The stopped-flow technique was also used to monitor the fluorescence intensity of the remaining tryptophans in GLA and its mutants during refolding and unfolding by dilution with buffers containing various final GdnHCl concentrations. Figure 6A represents the denaturant dependence of the initial and final fluorescence intensities for wt GLA. The U to N transition obtained from these kinetic experiments is comparable to that from the equilibrium experiments. Below 1.5 M GdnHCl, the initial amplitude deviates from the intensity expected for the fully unfolded protein. This refers to an unresolved folding event during the dead time and reflects the presence of a burst phase intermediate. The chevron plot (Figure 6B) shows a minimum that coincides with the midpoint of the N to U transition derived from the final intensities observed in the kinetic traces. As can be seen in Figure 6, the refolding and unfolding behavior of our wt GLA is completely identical with that of authentic GLA, derived from goat milk.

Figure 7 shows the initial and final fluorescence intensities and the chevron plots for the W26F, W60F, W104F, and W118F mutants. Once refolding has occurred, in each case

Table 1: Equilibrium Denaturation Parameters of Trp Mutants of GLA

	$\Delta G_{NU}^{H_2O}$ (kJ mol^{-1})	m_{NU} (kJ mol^{-1} M^{-1})	$\Delta G_{NI}^{H_2O}$ (kJ mol^{-1})	m_{NI} (kJ mol^{-1} M^{-1})	$\Delta G_{IU}^{H_2O}$ (kJ mol^{-1})	m_{IU} (kJ mol^{-1} M^{-1})
wt	42.84 ± 1.33	12.56 ± 0.95				
W118F	43.50 ± 2.64	12.80 ± 1.96				
W104F	33.34 ± 2.02	11.73 ± 1.62				
W60F	37.53 ± 1.86	11.09 ± 0.92	20.82 ± 3.56	6.33 ± 0.41	16.71 ± 4.01	4.76 ± 1.01
W26F	32.80 ± 1.89	11.75 ± 0.95	17.50 ± 2.33	6.91 ± 0.82	15.30 ± 2.29	4.84 ± 0.97

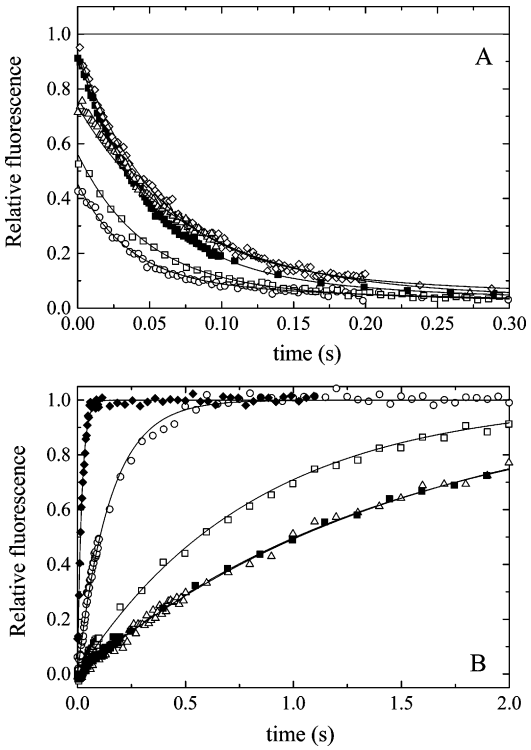

FIGURE 5: Time course of (A) kinetic refolding after dilution from 6 to 0.54 M GdnHCl and (B) kinetic unfolding after addition of GdnHCl to a final concentration of 5.05 M for wild-type GLA (■) and for mutants W118F (□), W104F (○), W60F (△), and W26F (◆) monitored by stopped-flow fluorescence. The solid lines represent double-exponential (A) and single-exponential (B) fits through the experimental data. The parameters are summarized in Table 1.

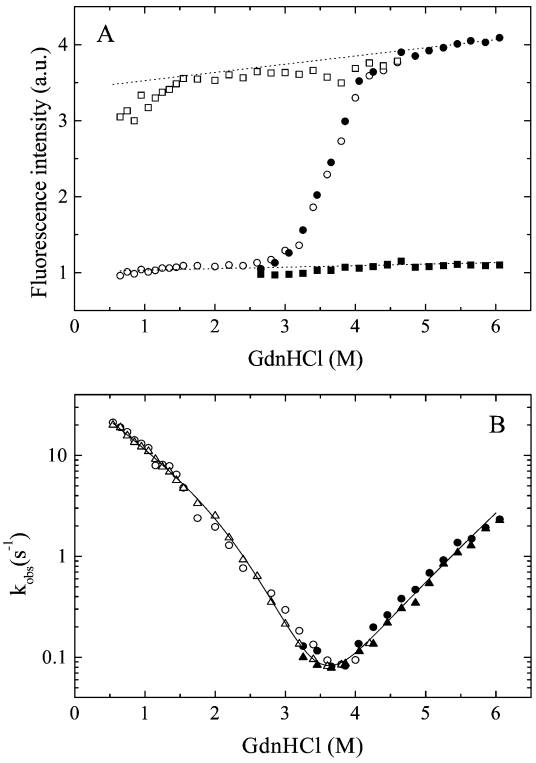

FIGURE 6: Dependence of the kinetics of refolding and unfolding of wt GLA on the GdnHCl concentration at pH 7.5 and 25 °C. In panel A, the initial (□ and ■) and final (○ and ●) values of the fluorescence intensity during folding (□ and ○) and unfolding (■ and ●) are shown. The dotted line at the top of the figure shows the fluorescence intensity expected for the unfolded state, assuming that it changes linearly with denaturant concentration. The dotted line at the bottom has the same meaning, but this time for the native state. In panel B, the observed rate constants of folding (○ and △) and unfolding (● and ▲) are shown for wt GLA (○ and ●) and authentic GLA (△ and ▲) as a function of the final GdnHCl concentration. The solid line through the data of wt GLA is the result of the fit with the three-state on-pathway model with the c^2 term in the unfolding limb.

Table 2: Refolding Rates of GLA and Its Mutants in 0.54 M GdnHCl (pH 7.5), 20 mM Tris, 10 mM Ca^{2+}, and 80 mM Na^+ at 25 °C

	A_1[a] (%)	$k_{1,ref}$ (s^{-1})	A_2[a] (%)	$k_{2,ref}$ (s^{-1})	burst phase (%)	k_{unf}[b] (s^{-1})
authentic	88.5	19.5	11.5	2.21	7.3	0.54
wt	90.4	20.8	9.6	2.06	7.3	0.68
W118F	89.3	21.7	10.7	2.86	44.3	1.23
W104F	80.1	28.2	19.9	3.06	54.9	4.89
W60F	86.7	11.9	13.3	2.01	26.4	0.65
W26F	89.3	17.5	10.7	2.57	6.3	68.8

[a] A_1 and A_2 represent the fractional amplitudes of the refolding signal after the dead time in a biexponential analysis. [b] The unfolding rates are determined in 5.05 M GdnHCl.

a burst phase is detected by the deviation of the initial intensity from the extrapolated fluorescence intensity of the unfolded protein. Among the two phases observed in the refolding process, the fastest one has the larger amplitude and its rate constant decreases with an increase in denaturant concentration. The rate constant of the slower phase, however, is nearly independent of the GdnHCl concentration. This type of behavior refers to a slow isomerization around an X−Pro bond rather than to a specific folding event (*18*, *26*). In the chevron plots, the denaturant dependence of the observed rates deviates from linearity at low (<1−2 M) and at high (>4.5−5 M) GdnHCl concentrations. The missing amplitude at the start of the refolding and the nonlinear rate profile with a decreasing slope at low GdnHCl concentrations are inconsistent with a simple two-state folding process and suggest the involvement of transient intermediates during the refolding process (*12*, *14*, *15*). The unfolding rate increases linearly with an increase in denaturant concentration up to approximately 5 M GdnHCl but deviates from linearity under stronger unfolding conditions. This rollover in the unfolding limb has been suggested to possibly originate from the effect of viscosity (*30*, *31*). As solutions with high concentrations of GdnHCl are significantly viscous (*32*), they therefore could diminish the value of the apparent rate constant. To estimate the effect of GdnHCl viscosity, the observed rates

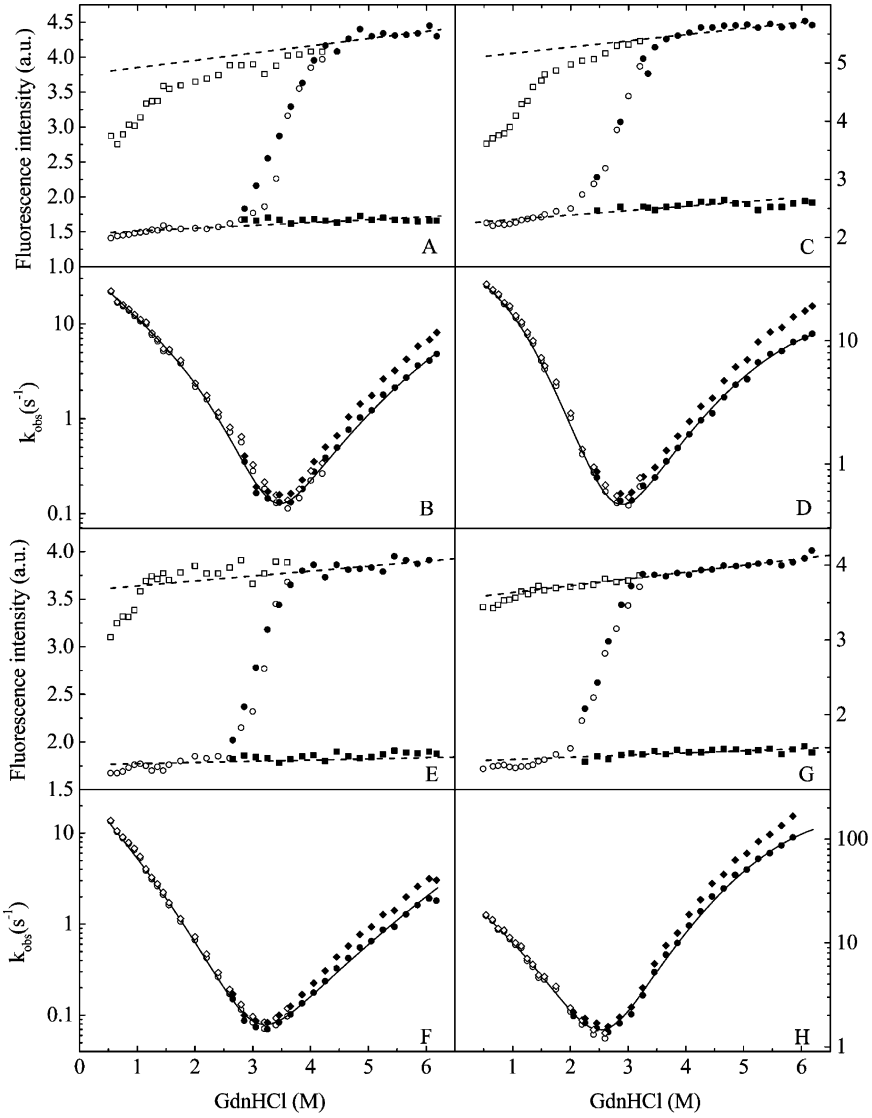

FIGURE 7: Initial (□ and ■) and final (○ and ●) values of fluorescence intensity and observed rates (○ and ●) obtained from kinetic folding (□ and ○) and unfolding (■ and ●) experiments on W118F (A and B), W104F (C and D), W60F (E and F), and W26F (G and H). The diamonds in panels B, D, F, and H are the observed rates of folding (◇) and unfolding (◆), corrected for the intrinsic effects of the viscosity of the GdnHCl solution (see the text). In the latter panels, the fit to the three-state on-pathway model with the c^2 term in the unfolding limb is shown as a solid line. The experimental conditions are the same as for wt GLA.

were corrected as described by Jacob and Schmid (*33*). This correction reduces the curvature in the unfolding limb, but the curvature does not disappear entirely (Figure 7). Therefore, it is very unlikely that the curvature in the chevron plots is uniquely caused by effects induced by specific experimental conditions. It rather could be related to the intrinsic folding behavior. On the other hand, it must be remembered that the unfolding process evolves in a monoexponential way and that no fluorescence intensity change is observed during the dead time.

Modeling of the Kinetic Results. It has been proposed recently that the chevron plots, which represent the folding and unfolding kinetics of authentic GLA, can adequately be described by a three-state model in which the intermediate is assumed to be formed on-pathway within the dead time of the stopped-flow experiment (*18*). The unfolded state and the intermediate state equilibrate with each other in a very fast but obligatory step with an equilibrium constant K_{UI} ($=k_{UI}/k_{IU}$). In general, the rate constant λ_1 ($=k_{UI}+k_{IU}$) related to this process cannot be measured directly. In this on-pathway model, the rate constant that corresponds to the I to N transition is rate-limiting and can be described by

$$\lambda_2 = \frac{K_{UI}}{1+K_{UI}}k_{IN} + k_{NI} \quad (3)$$

The major rate constant that is observed in our measurements corresponds to this quantity λ_2.

The folding and unfolding rate constants can be described by eqs 4 and 5, respectively.

$$k_f = f_I k_{IN} = \frac{K_{UI}}{1+K_{UI}}k_{IN} \quad (4)$$

$$k_u = k_{NI} \quad (5)$$

The three quantities ln k_{IN}, ln k_{NI}, and K_{UI} are presumed to vary linearly with the GdnHCl concentration. As a conse-

Table 3: Kinetic Parameters Derived by Using a Three-State On-Pathway Model with the c^2 Term for wt GLA and Trp Mutants at pH 7.5 and 25 °C

	wt GLA	W118F	W104F	W60F	W26F
$\Delta G_{UI}^{H_2O}$ (kJ/mol)	-12.20 ± 1.10	-11.74 ± 1.41	-6.29 ± 1.04	-5.45 ± 1.02	-2.70 ± 0.90
m_{UI} (kJ mol^{-1} M^{-1})	5.17 ± 0.42	5.07 ± 0.4	5.85 ± 0.22	3.25 ± 0.71	3.25 ± 0.43
$k_{IN}^{H_2O}$ (s^{-1})	42.3 ± 1.4	43.1 ± 1.2	43.78 ± 2.08	35.0 ± 1.6	43.40 ± 1.60
$m_{IN}^{\ddagger}$ (kJ mol^{-1} M^{-1})	-3.08 ± 0.10	-3.08 ± 0.11	-0.98 ± 0.55	-3.84 ± 0.31	-1.62 ± 0.24
$k_{NI}^{H_2O}$ (s^{-1})	$(2 \pm 0.5) \times 10^{-4}$	$(1 \pm 0.8) \times 10^{-5}$	$(2.4 \pm 1.3) \times 10^{-4}$	$(2.3 \pm 1.1) \times 10^{-4}$	$(2.7 \pm 0.8) \times 10^{-4}$
$m_{IN}^{\ddagger}$ (kJ mol^{-1} M^{-1})	5.40 ± 1.2	7.87 ± 0.91	7.59 ± 0.72	4.64 ± 0.86	9.27 ± 0.51
b (kJ mol^{-1} M^{-2})	-0.15 ± 0.05	-0.42 ± 0.04	-0.53 ± 0.07	-0.15 ± 0.02	-0.65 ± 0.09
c_M (M)[a]	3.48	3.38	2.79	3.07	2.58
$\Delta G_{UN}^{H_2O}$ (kJ/mol)[b]	-42.52 ± 1.15	-49.59 ± 2.3	-36.30 ± 1.79	-35 ± 1.05	-32.40 ± 1.21
m_{UN} [c] (kJ mol^{-1} M^{-1})	13.13 ± 1.29	13.19 ± 0.99	11.47 ± 0.93	10.80 ± 1.15	10.79 ± 1.06
ϕ_I	–	-0.06	0.95	0.90	0.94
$\phi^{\ddagger}$	–	-0.07	0.96	0.84	0.93
$\beta^{\ddagger}$	0.63	0.62	0.63	0.66	0.50
β_I	0.39	0.38	0.54	0.30	0.33

[a] The c_M value is determined by the condition $k_f = k_u$. [b] $\Delta G_{UN}^{H_2O} = \Delta G_{UI}^{H_2O} - RT \ln(k_{IN}^{H_2O}/k_{NI}^{H_2O})$. [c] The m_{UN} value is calculated at the midpoint of the transition according to the equation $m_{UN} = m_{UI} - m_{IN}^{\ddagger} + m_u$.

quence, the $\lambda_2 = k_{obs}$ relation can be written as

$$k_{obs} = \frac{e^{-(\Delta G_{UI}^{H_2O} - m_{UI}c)/RT}}{1 + e^{-(\Delta G_{UI}^{H_2O} - m_{UI}c)/RT}} k_{IN}^{H_2O} e^{\frac{m_{IN}^{\ddagger} c}{RT}} + k_{NI}^{H_2O} e^{\frac{m_{NI}^{\ddagger} c}{RT}} \quad (6)$$

where $k_{ij}^{H_2O}$ values are the microscopic rate constants for the conversion from state i to state j in the absence of denaturant and $m_{ij}^{\ddagger}$ represents the dependence of k_{ij} on denaturant concentration. This type of analysis, which implies a linear dependence of ln k_{NI} on the denaturant concentration, leads to a linear behavior in the unfolding limb and to a constant value for $m_{NI}^{\ddagger}$. The data obtained for the different mutants, however, show a deviation of linearity in the unfolding limb (Figure 7). Such a curvature in the unfolding branch of a chevron plot has been seen in many other proteins and can often be related to a nonlinear dependence of ln k_{NI} on denaturant concentration (*34*−*41*):

$$\ln k_u = \ln k_{NI} = \ln k_{NI}^{H_2O} + \frac{m_{NI}^{\ddagger} c}{RT} + \frac{bc^2}{RT} \quad (7)$$

When eq 7 is taken into account, the theoretical model indeed better fits our experimental data, and the resulting kinetic parameters are summarized in Table 3.

The m value of the unfolding process is defined as the derivative of ln k_u to c and thus can be written as

$$m_u = m_{NI}^{\ddagger} + 2bc \quad (8)$$

The position of the intermediate state (β_I) and of the rate-limiting transition state ($\beta^{\ddagger}$) along the reaction coordinate can be obtained from the kinetic m values derived from the modeling as follows:

$$\beta_I = \frac{m_{UI}}{m_{UI} - m_{IN}^{\ddagger} + m_u} \quad (9)$$

$$\beta^{\ddagger} = \frac{m_{UI} - m_{IN}^{\ddagger}}{m_{UI} - m_{IN}^{\ddagger} + m_u} \quad (10)$$

The values of these parameters are calculated at the c_M of the wt protein (Table 3). The position of the transition state on the reaction coordinate is practically constant for all samples except for W26F. With regard to the position of the intermediate state, we also found a nearly constant value with the exception of that of W104F. Whether this movement of the transition state is due to continuous Hammond behavior across energy barriers (*37*, *42*) or to a change in the rate-limiting step of the reaction (*39*, *43*) remains to be further investigated by the analysis of a larger set of mutants.

φ Value Analysis. The structure of the transition states and the intermediate states that occur during the folding process may be inferred from the changes in the kinetics of folding upon mutation (*44*). This procedure, known as ϕ value analysis, makes use of the difference of the Gibbs free energy between the wild type and the mutant protein:

$$\Delta\Delta G_{UN}(c) = \Delta G_{UN}^{wt}(c) - \Delta G_{UN}^{mut}(c) \quad (11)$$

The ϕ value of the kinetic intermediate state is then defined as

$$\phi_I = \Delta\Delta G_{UI}/\Delta\Delta G_{UN} \quad (12)$$

and that of the transition state as

$$\phi^{\ddagger} = \frac{\Delta\Delta G_{UI} + \Delta\Delta G_{ITS}}{\Delta\Delta G_{UN}} \quad (13)$$

A ϕ value of 0 for the intermediate state means that, upon mutation, the energy of the intermediate state is perturbed by the same amount as that of the denatured state. A ϕ value of 1 means that the intermediate state is perturbed by the same amount as the native state. Therefore, a ϕ of 0 refers to a structure at the mutation site that is as unfolded as it is in the denatured state, while a ϕ of 1 refers to a structure as much folded as in the native state.

The ϕ values of all the Trp mutants were calculated with eqs 11−13 and are summarized in Table 3. The $\Delta\Delta G_{ITS}$ is determined from the $k_{IN}^{H_2O}$ values for the wild type and the mutants as

$$\Delta\Delta G_{ITS} = -RT \ln(k_{IN}^{wt}/k_{IN}^{mut}) \quad (14)$$

The ϕ_I values of W26F, W60F, and W104F are close to 1 which means that, when Trp26, Trp60, or Trp104 is replaced with Phe, the kinetic intermediate and the native state are destabilized by the same amount. In other words, in these proteins the intermediate state at the mutation site has a native character. In contrast, the ϕ_I value for the intermediate of W118F is 0, reflecting the fact that in the intermediate state the mutation site is still unfolded. Similar results were found for $\phi^{\ddagger}$, indicating that the mutation of Trp118 has no specific effect on the transition state.

DISCUSSION

Equilibrium Unfolding of the Trp Mutants. The replacement of Trp118 with Phe does not affect the stability of the protein within the error limit, while the mutation of Trp104 obviously reduces the stability of the native conformation (Table 1). For both proteins, however, the unfolding transition preserves the two-state character observed in wild-type GLA. On the other hand, the replacement of Trp60 or Trp26 in GLA makes the equilibrium unfolding behavior more complex. The noncoincidence of the near-UV CD or fluorescence transition curve and the far-UV CD transition curve (Figure 4) clearly shows that the disruption of the secondary and tertiary structure is uncoupled, as in the case of authentic α-lactalbumin at low pH or in the Ca^{2+}-free form. The breakdown of the global cooperativity detected for these Trp mutants demonstrates that well-chosen point mutations can also be used to enhance the population of a partially folded form. Similar noncoincident transition curves where obtained for nine other mutants of GLA under somewhat different experimental conditions (*26*).

It is well-known that the native state of all α-lactalbumins, goat α-lactalbumin included, is stabilized by the addition of Ca^{2+} ions and also that this Ca^{2+} form undergoes a cooperative two-state unfolding transition between the native and unfolded state (*45*). A molten globule intermediate only appears at low pH or in the apo form. For GLA, this intermediate has been observed in the absence of Ca^{2+} ions at neutral pH in 1.5 M GdnHCl or in the presence of 10 mM Ca^{2+} at pH 4.5 in 3.1 M GdnHCl (*18*). It is thus remarkable that a molten globule state can also be induced by a point mutation in the presence of a high Ca^{2+} concentration at neutral pH, as observed in this study for W60F and W26F. It is interesting to compare the thermodynamic parameters obtained from the analysis of the equilibrium unfolding curves of W60F and W26F (Table 1) with the corresponding parameters of authentic GLA at pH 4.5 that have been obtained in our previous study (*18*). The thermodynamic stability of the molten globule state compared to that of the fully unfolded state ($\Delta G_{IU}^{H_2O}$) for GLA in the presence of 10 mM Ca^{2+} at pH 4.5 and the $\Delta G_{IU}^{H_2O}$ values for the W26F and the W60F mutants are very similar (∼16 kJ/mol). Furthermore, the corresponding m_{IU} values are on the same order of magnitude (Table 1). These findings strongly suggest the similarity of both equilibrium intermediates. For these Trp mutants and for authentic GLA at pH 4.5, the calculated $\Delta G_{NU}^{H_2O}$ values (32.8, 37.5, and 28.4 kJ/mol, respectively) are markedly lower than the corresponding value of wt GLA at pH 7.5 (42.84 kJ/mol), indicating that the native state in the former samples is destabilized (*18*). The destabilization induced by mutation, however, is less drastic than that induced by lowering the pH.

Effect of Trp Mutation on the Kinetic Intermediate and the Transition State. From Figures 6 and 7 it is clear that wild-type GLA and the four mutants refold through a kinetic intermediate state. This state, however, is obviously not the same for the different proteins as the degree to which it is formed and the rate at which it is formed vary for each sample (Table 2).

Moreover, the kinetic parameters related to the intermediate state show the distinctive influence of the respective mutations (Table 3). For W118F, the $\Delta G_{UI}^{H_2O}$ and m_{UI} values are similar to those obtained for wt GLA, and thus, the kinetic intermediate is hardly affected by the mutation of Trp118 to Phe. The ϕ_I value for this mutant is near zero, indicating that the mutation affects the unfolded and intermediate state in the same way.

Mutating Trp to Phe at position 104 or 60 conserves the burst phase amplitude but results in a destabilization of the kinetic intermediate ($\Delta\Delta G_{UI}^{wt-mut}$) of 5.91 or 6.75 kJ/mol, respectively. These destabilizations of the intermediate state are on the same order of magnitude as those of the native state: indeed, $\Delta\Delta G_{UN}^{wt-mut}$ equals 6.22 and 7.52 kJ/mol, respectively (Table 3). The ϕ_I value equals 0.95 for the kinetic intermediate of W104F and 0.90 for W60F.

The W26F mutant folds through a highly destabilized kinetic intermediate. Both the burst phase signal and the rollover of the chevron plot are hardly detectable at low denaturant concentrations (Figure 7G,H). For this mutant, the stability of the kinetic intermediate (ΔG_{UI} = 2.70 kJ/mol) is substantially lower than that for wt (ΔG_{UI} = 12.20 kJ/mol). The *m* value of the kinetic intermediate (m_{UI}) in W26F is less than that for the wt (Table 3), and the burst phase signal is around 6% of the total signal change. The effect of this mutation on the kinetic intermediate ($\Delta\Delta G_{UI}$ = 9.50 kJ/mol) is similar to the effect on the native state ($\Delta\Delta G_{UN}$ = 10.12 kJ/mol). The latter values result in a ϕ value for the intermediate equal to 0.94. From these observations, important conclusions about the structure of the kinetic intermediate can be drawn. A plot of $\Delta\Delta G_{UN}$ versus $\Delta\Delta G_{UI}$ for the different proteins (not shown) shows a linear relationship with a slope of 0.49 and a correlation coefficient *R* of 0.98. This means that each mutation affects the energy levels of the kinetic intermediate state and that of the native state by the same amount, and therefore, the stabilities of the intermediate and of the native state change in the same way. Different ΔG_{UI} values for the different samples reflect different stabilities of the kinetic intermediate referring to specific side chain interactions. In their analysis of the free energy state of a series of point mutants of GLA, Saeki et al. (*26*) found no significant correlation between $\Delta\Delta G_{UN}$ and $\Delta\Delta G_{UI}$ where the $\Delta\Delta G_{UI}$ values were distributed in a narrow range around zero. These results, however, are obtained by equilibrium measurements, whereas our conclusions are based on kinetic experiments. It therefore must be considered that the equilibrium and kinetic intermediates must be distinguished from each other. The fact that the kinetic and equilibrium intermediates are not identical, although they have some common characteristics, was previously reported for LYLA1, a chimeric protein resulting from the transplantation of a part of bovine α-lactalbumin into the homologous position in human lysozyme (*46*).

Also, the effect of Trp substitution on the transition state can be derived from possible changes in the folding kinetics of the protein. The GdnHCl dependence of the rate constants for W118F, W104F, W60F, and W26F is depicted in Figure 7, together with the theoretical fit by the on-pathway three-state model. For W118F, W104F, and W26F, the microscopic rate constant extrapolated to zero denaturant concentration, $k_{IN}^{H_2O}$, is essentially the same as that for wild-type GLA (Table 3), implying that the transition state free energy barrier of the I to N transition in these mutants also remains the same. For the W60F mutant, the $k_{IN}^{H_2O}$ value differs somewhat from that of the wild type, but even in this case, no significant effect on the transition state free energy barrier is found.

Effect of Hydrophobicity and Steric Packing on the Kinetic Intermediate and on the Transition State. The ϕ value analysis for W104F, W60F, and W26F reveals that both ϕ_I and $\phi^{\ddagger}$ are close to 1, indicating that these residues are making nativelike interactions in the kinetic intermediate as well as in the transition state. This confirms our conclusion that for each of these mutants, the kinetic intermediate, the transition state, and the native state are destabilized in the same way.

In contrast to our findings, Saeki et al. (*26*) have demonstrated that in a mutant where Trp60 is substituted with alanine the nativelike interactions around the mutation site are not yet formed in the transition state. The latter mutation does preserve the hydrophobic nature of the site but is more drastic with regard to the shape and size of the mutated residue. The lack of native character in the intermediate state which was observed for W60A suggests that hydrophobicity is not the only driving force for folding and that other effects, such as steric packing, can play a major role. Although the hydrophobic character of the mutation site in W60A is conserved, the alanine residue is not able to achieve the nativelike interactions effectuated by the Trp residue in that position.

An analogous reasoning can be carried out with regard to W26F. The substitution of Trp with Phe at position 26 preserves the hydrophobic nature and introduces only a small steric change at the mutation site. Nevertheless, from all our samples, this mutation is the most destabilizing one. The intermediate was destabilized by 9.50 kJ/mol, and the total change in stability is 10.12 kJ/mol. Subtle changes in packing and even small steric effects thus can have a considerable influence on local helix propensity, on the stability of the various states, and on the folding pathway. Recently, a similar but even more pronounced mutagenic effect has been seen for the Y120W mutant of Bet v 1 (*47*). These authors suggest that this single-point mutation, which compared to Tyr introduces an extra imidazole ring, has caused such a severe steric clash that presumably the intermediate is sufficiently destabilized to eliminate its accumulation.

The ϕ value analysis for the W118F mutant reveals that ϕ_I and $\phi^{\ddagger}$ have values close to 0, which means that the structure around this mutation site is organized neither in the kinetic intermediate nor in the transition state. The region around residue 118 at the C-terminus, therefore, is not involved in the initial phase of the folding process. This is in complete agreement with previous studies where it has been shown that the structure around the 6−120 disulfide bond is not yet organized in the transition state during refolding (*48*). Another rigorous study of the stability and folding of recombinant GLA has shown that the folding initiation site is not located in the N-terminal region (*20*). The latter considerations together with our conclusions regarding the various Trp mutants give support to the observation that the structure around the Ca^{2+}-binding site is already organized in the transition state and thus is part of the folding initiation site (*8*, *26*).

REFERENCES

1. Ptitsyn, O. B., Pain, R. H., Semitsonov, O. V., Zerovnik, E., and Razgulyaev, O. I. (1990) Evidence for a molten globule state as a general intermediate in protein folding, *FEBS Lett. 262*, 20−24.
2. Sanchez, I. E., and Kiefhaber, T. (2003) Evidence for sequential barriers and obligatory intermediates in apparent two-state folding, *J. Mol. Biol. 325*, 367−376.
3. Radford, S., Dobson, C., and Evans, P. (1992) The folding of hen lysozyme involves partially structured intermediates and multiple pathways, *Nature 358*, 302−307.
4. Van Dael, H. (1998) Chimeras of human lysozyme and α-lactalbumin: An interesting tool for studying partially folded states during protein folding, *Cell. Mol. Life Sci. 54*, 1217−1230.
5. Gunasekaran, K., Eyles, S. J., Hagler, A. T., and Gierasch, L. M. (2001) Keeping it in the family: Folding studies of related proteins, *Curr. Opin. Struct. Biol. 11*, 83−93.
6. Acharya, K. R., Stuart, D. I., Walker, N. P., Lewis, M., and Phillips, D. C. (1989) Refined structure of baboon α-lactalbumin at 1.7 Å resolution. Comparison with C-type lysozyme, *J. Mol. Biol. 208*, 99−127.
7. Pike, A. C. W., Brew, K., and Acharya, K. R. (1996) Crystal structures of guinea-pig, goat and bovine α-lactalbumin highlight the enhanced conformational flexibility of regions that are significant for its action in lactose synthase, *Structure 4*, 691−703.
8. Kuwajima, K. (1989) The molten globule state as a clue for understanding the folding and cooperativity of globular-protein structure, *Proteins 6*, 87−103.
9. Chyan, C. L., Wormald, C., Dobson, C. M., Evans, P. A., and Baum, J. (1993) Structure and stability of the molten globule state of guinea-pig α-lactalbumin: A hydrogen exchange study, *Biochemistry 32*, 5681−5691.
10. Arai, M., and Kuwajima, K. (1996) Rapid formation of a molten globule intermediate in refolding of α-lactalbumin, *Folding Des. 1*, 275−287.
11. Yoda, T., Saito, M., Arai, M., Horii, K., Tsumoto, K., Matsushima, M., Kumagai, I., and Kuwajima, K. (2001) Folding−unfolding of goat α-lactalbumin studied by stopped-flow circular dichroism and molecular dynamics simulations, *Proteins 42*, 49−65.
12. Ikeguchi, M., Kuwajima, K., Mitani, M., and Sugai, S. (1986) Evidence for the identity between the equilibrium unfolding intermediate and a transient folding intermediate: A comparative study of the folding reactions of α-lactalbumin and lysozyme, *Biochemistry 25*, 6965−6972.
13. Redfield, C. (2004) Using nuclear magnetic resonance spectroscopy to study molten globule states of proteins, *Methods 34*, 121−132.
14. Matouschek, A., Kellis, J. T., Jr., Serrano, L., Bycroft, M., and Fersht, A. R. (1990) Transient folding intermediates characterized by protein engineering, *Nature 346*, 440−445.
15. Khorasanizadeh, S., Peters, I. D., and Roder, H. (1996) Evidence for a three-state model of protein folding from kinetic analysis of ubiquitin variants with altered core residues, *Nat. Struct. Biol. 3*, 193−205.
16. Spudich, G. M., Miller, E. J., and Marqusee, S. (2004) Destabilization of the *Escherichia coli* RNase H kinetic intermediate: Switching between a two-state and three-state folding mechanism, *J. Mol. Biol. 335*, 609−618.
17. Friel, C. T., Beddard, G. S., and Radford, S. E. (2004) Switching two-state to three-state kinetics in the helical protein Im9 via the optimisation of stabilising non-native interactions by design, *J. Mol. Biol. 342*, 261−273.
18. Chedad, A., and Van Dael, H. (2004) Kinetics of folding and unfolding of goat α-lactalbumin, *Proteins 57*, 345−356.

19. Ishikawa, N., Chiba, T., Chen, L. T., Shimizu, A., Ikeguchi, M., and Sugai, S. (1998) Remarkable destabilization of recombinant α-lactalbumin by an extraneous N-terminal methionyl residue, *Protein Eng. 11*, 333−335.
20. Chaudhuri, T. K., Horii, K., Yoda, T., Arai, M., Nagata, S., Terada, T. P., Uchiyama, H., Ikura, T., Tsumoto, K., Kataoka, H., Matsushima, M., Kuwajima, K., and Kumagai, I. (1999) Effect of the extra N-terminal methionine residue on the stability and folding of recombinant α-lactalbumin expressed in *Escherichia coli*, *J. Mol. Biol. 285*, 1179−1194.
21. Vanhooren, A., Chedad, A., Farkas, V., Majer, Z., Joniau, M., Van Dael, H., and Hanssens, I. (2005) Tryptophan to phenylalanine substitutions allow differentiation of short and long range conformational changes during denaturation of goat α-lactalbumin, *Proteins 60*, 118−130.
22. Loewenthal, R., Sancho, J., and Fersht, A. R. (1991) Fluorescence spectrum of barnase-contributions of three tryptophan residues and a histidine related pH dependence, *Biochemistry 30*, 6775−6779.
23. Locke, B. C., MacInnis, J. M., Qian, S. J., Gordon, J. I., Li, E., Fleming, G. R., and Yang, N. C. (1992) Fluorescence studies of rat cellular retinol binding protein-II produced in *E. coli*: An analysis of four tryptophan substitution mutants, *Biochemistry 31*, 2376−2383.
24. Pace, C. N. (1986) Determination and analysis of urea and guanidine hydrochloride denaturaion curves, *Methods Enzymol. 131*, 266−280.
25. Mizuguchi, M., Arai, M., Ke, Y., Nitta, K., and Kuwajima, K. (1998) Equilibrium and kinetics of the folding of equine lysozyme studied by circular dichroism spectroscopy, *J. Mol. Biol. 283*, 265−277.
26. Saeki, K., Arai, M., Yoda, T., Nakao, M., and Kuwajima, K. (2004) Localized nature of the transition-state structure in goat α-lactalbumin folding, *J. Mol. Biol. 341*, 589−604.
27. Woody, R. W. (1994) Contributions of tryptophan side chains to the far-ultraviolet circular dichroism of proteins, *Eur. Biophys. J. 23*, 253−262.
28. Van Dael, H., Chedad, A., Vanhooren, A., and Hanssens, I. (2005) Influence of experimental conditions and Trp mutations on the stability and the folding characteristics of goat α-lactalbumin, *J. Mol. Struct. 744*−*747*, 155−160.
29. Eftink, M. R. (2000) Use of fluorescence spectroscopy as thermodynamics tool, *Methods Enzymol. 323*, 459−473.
30. Karplus, M., and Weaver, D. L. (1976) Protein-folding dynamics, *Nature 260*, 404−406.
31. Jacob, M., Schindler, T., Balbach, J., and Schmid, F. X. (1997) Diffusion control in an elementary protein folding reaction, *Proc. Natl. Acad. Sci. U.S.A. 94*, 5622−5627.
32. Kawahara, K., and Tanford, C. (1966) Viscosity and density of aqueous solutions of urea and guanidine hydrochloride, *J. Biol. Chem. 241*, 3228−3232.
33. Jacob, M., and Schmid, F. X. (1999) Protein folding as a diffusional process, *Biochemistry 38*, 13773−13779.
34. Silow, M., and Oliveberg, M. (1997) High energy channelling in protein folding, *Biochemistry 36*, 7633−7637.
35. Clarke, J., Hamill, S. J., and Johnson, C. M. (1997) Folding and stability of a fibronectin type III domain of human tenascin, *J. Mol. Biol. 270*, 771−778.
36. Dalby, P. A., Oliveberg, M., and Fersht, A. R. (1998) Movement of the intermediate and rate determining transition state of barnase on the energy landscape with changing temperature, *Biochemistry 37*, 4674−4679.
37. Otzen, D. E., Kristensen, O., Proctor, M., and Oliveberg M. (1999) Structural changes in the transition state of protein folding: Alternative interpretations of curved chevron plots, *Biochemistry 38*, 6499−6511.
38. Fersht, A. R. (2000) A kinetically significant intermediate in the folding of barnase, *Proc. Natl. Acad. Sci. U.S.A. 97*, 14121−14126.
39. Bachmann, A., and Kiefhaber, T. (2001) Apparent two-state Tendamistat folding is a sequential process along a defined route, *J. Mol. Biol. 306*, 375−386.
40. Engman, K. C., Sandberg, A., Leckner, J., and Karlsson, B. G. (2004) Probing the influence on folding behaviour of structurally conserved core residues in *P. aeruginosa* apo-azurin, *Protein Sci. 13*, 2706−2715.
41. Sandberg, A., Leckner, J., and Karlsson, B. G. (2004) Apo-azurin folds via an intermediate that resembles the molten globule, *Protein Sci. 13*, 2628−2638.
42. Sanchez, I. E., and Kiefhaber, T. (2003) Hammond behaviour versus ground-state effects in protein folding: Evidence for narrow free energy barriers and residual structure in unfolded states, *J. Mol. Biol. 327*, 867−884.
43. Bollen, Y. J. M., Sanchez, I. E., and van Mierlo, C. P. M. (2004) Formation of on- and off-pathway intermediates in the folding kinetics of *Azotobacter vinelandii* apoflavodoxin, *Biochemistry 43*, 10475−10489.
44. Fersht, A. R. (1999) *Structure and mechanism in protein science: A guide to enzyme catalysis and protein folding*, p 631, W. H. Freeman and Co., New York.
45. Ikeguchi, M., Kuwajima, K., and Sugai, S. (1986) Ca^{2+}-induced alteration in the unfolding behaviour of α-lactalbumin, *J. Biochem. 99*, 1191−1201.
46. Haezebrouck, P., Noyelle, K., Joniau, M., and Van Dael, H. (1999) Kinetic and equilibrium intermediate states are different in LYLA1, a chimera of lysozyme and α-lactalbumin, *J. Mol. Biol. 293*, 703−718.
47. Mogensen, J. E., Ipsen, H., Holm, J., and Otzen, D. (2004) Elimination of a misfolded folding intermediate by a single point mutation, *Biochemistry 43*, 3357−3367.
48. Ikeguchi, M., Fujino, M., Kato, M., Kuwajima, K., and Sugai, S. (1998) Transition state in the folding of α-lactalbumin probed by the 6−120 disulfide bond, *Protein Sci. 7*, 1564−1574.
49. Guex, N., and Peitsch, M. C. (1997) Swiss-model and the Swiss-PDB viewer: An environment for comparative protein modelling, *Electrophoresis 18*, 2714−2723.

BI0512400